CHARACTERISATION OF OPTICAL PAYLOADS AND POTENTIAL EJECTA REACTIONS (COPPER)

James Beck[(1)], Ian Holbrough [(1)], Jim Merrifield[(2)], Erhard Kaschnitz[(3)], Martin Jackson[(4)], Yunus Azakli[(4)], Peter Doel[(5)], Berend Winter[(5)], Paul Bingham[(6)], Jess Rigby[(6)], James Eales[(6)], Thorn Schleutker[(7)], Oliver Hohn[(7)], Benoit Bonvoisin[(8)]

[(1)] Belstead Research Limited, 387 Sandyhurst Lane, Ashford, TN25 4PF, UK
[(2)]Fluid Gravity Engineering Limited, The Old Coach House, Emsworth, PO10 7DX, UK
[(3)]Österreichisches Gießerei-Institut, Parkstrasse 21, 8700 Leoben, Austria
[(4)]University of Sheffield, Department of Material Science and Engineering, Mappin Street, Sheffield, S1 3JD, UK
[(5)]University College London, Gower Street, London WC1E 6BT, UK
[(6)]Sheffield Hallam University, City Campus, Howard Street, Sheffield, S1 1WB, UK
[(7)]Deutsches Zentrum für Luft- und Raumfahrt, Linder Höhe, 51147 Cologne, Germany
[(8)]ESA-ESTEC, Keplerlaan 1, Postbus 299, 2200 AG Noordwijk, The Netherlands

ABSTRACT

The demisability of optical payloads is challenging due to the high performance materials used. Two high ground risk aspects, glass materials used in lenses and mirrors, and titanium bipods were tested and carefully modelled in this work.

A number of previous works have attempted to assess the demisability of glass materials, in particular Zerodur, although little material demise testing has been performed. In this work, a set of material demisability tests were performed in conjunction with an assessment of the glass viscosity-temperature curve. The tests demonstrate that, although material deformation can be observed earlier, material removal is driven by the viscosity of the glass, and not by a melting temperature. The rate of material removal can be correlated directly with the viscosity, and a model has been derived which successfully rebuilds the material loss in a set of tests performed in the DLR L2K high enthalpy wind tunnel. This model, implemented in SAMj, demonstrates that Zerodur is significantly less demisable than estimated by current models, which perform poorly against the test data.

A titanium bipod designed to support an 8kg mirror was also tested in the L2K facility, and the demise of the bipod was clearly demonstrated to be linked to the length scales of the different parts of the bipod. The cutouts which enable the flexure of the bipod melted first, promoting a fragmentation of the bipod into smaller parts, and the relatively small length scale of the legs and foot resulted in the demisability being relatively good. Using 3D printing, a set of demise enhancing features were tested. A hollow version of the bipod, and then a bipod with a set of holes allowing the flow to pass through, were tested. Both models satisfied the load and flexure requirements of the original bipod design. The hollow bipod was seen to improve the demisability slightly due to the lower mass of the object. The design with holes, however, demonstrated a substantial improvement in the demisability of the bipod, consistent with a halving of the length scale of the object. This suggests that flow holes are an effective design-for-demise technique, and it is strongly recommended that more research is put into this concept.

Another demisability aspect, the interaction of molten aluminium ejecta on hot titanium and steel surfaces was also investigated, but showed no indication of causing significant energetic reactions to enhance demise.

1. INTRODUCTION

Three separate aspects are considered for testing and modelling within this activity. The first is the possibility of reactions between hot, molten metal ejecta from melting parts, and hot low demisability metal surfaces. In particular, the reactions between molten aluminium ejecta and steel or titanium surfaces are considered.

The second aspect examined is the demise of glass materials. Two specific materials, fused silica and Zerodur are tested with the intention of producing a general model for the demise of glass materials. The demise is expected to be driven by the viscosity of the material, and thus the mass loss rate is expected to be controlled by the surface temperature.

The third aspect is the design of demisable bipods for the support of optical instruments. Here, a baseline design in titanium is produced and tested. The results of this test are analysed in order to produce two designs with improved demisability. Both these designs have to satisfy the mechanical requirements of the original design. Models are derived to capture the demise behaviour of the baseline, and attempt to capture the demise behaviour of the demisable alternatives.

2. EJECTA REACTIONS

A theoretical investigation into possible thermite, intermetallic, gasless combustion and oxidation reactions suggested that there was little evidence that significant energy would be released in the interaction of aluminium melt with hot titanium or steel surfaces. This was investigated further in two testing campaigns.

2.1 Laboratory Testing

To replicate the ejecta interaction at high temperatures and under low oxygen partial pressures (backfilled with argon), an Arcast SC100 strip casting machine at the University of Sheffield, originally designed for melt spinning, was adapted in order to enable aluminium ejecta to drop onto heated titanium alloy, Ti64 (Ti-6Al-4V), and stainless steel (316L) sheet. The Arcast has been adapted in two key areas. The positioning of the crucible holder and induction coil were moved from the copper melt spinning wheel to allow molten aluminium to be dropped from a height of approx. 35 cm (see Figure 1). Also, a 350 W resistant heating furnace using Kanthal A wire and alumina refractory bricks was designed and built in order to heat and maintain a constant temperature up to 1000°C for titanium/steel sheet substrate.

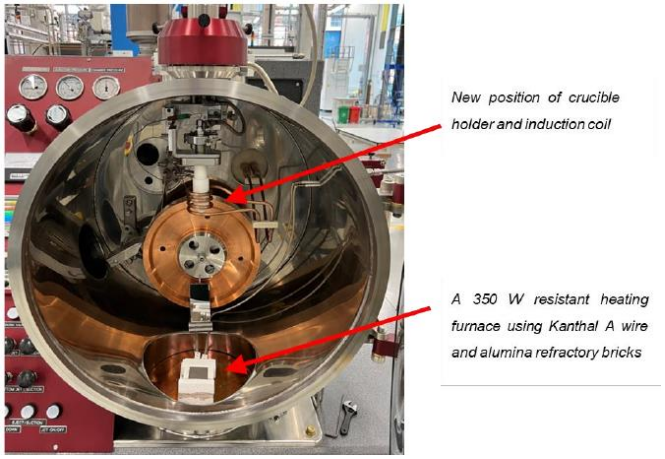

Figure 1: Strip Caster with Modifications

High purity aluminium was dropped at 750-800^{0}C from the Boron Nitride crucible. The substrates of Ti6Al4V and stainless stell 316L were heated to 850^{0}C and 1000^{0}C prior to dropping the molten aluminium.

Aluminium ejecta test on both 316L and Ti6Al4V alloys showed that the reaction of aluminium and these substrate materials was not severe and affected only the very surface of the substrates. For both substrate materials, further dissolution was inhibited by the formation of intermetallic phases at the interface.

2.2 Wind Tunnel Tests

The testing of the ejecta was performed in the DLR L2K facility, and proved to be extremely challenging. Three different set-ups for the experiment were used, finally resulting in a good deposition of aluminium melt on a hot titanium surface.

The ejecta tests make use of two primary types of components besides the wind tunnel itself – sacrificial parts and targets. Each sacrificial part comprises a cone or cylinder made of pure aluminium and is positioned downstream of the inlet nozzle in the L2K facility test chamber. A sacrificial part's position may be adjusted between tests using an articulated arm to which it is fixed. The targets are constructed from sheets of grade 2 titanium measuring 50mm in width and either 1 or 2mm in thickness. The final setup is shown in Figure 2, and uses aluminium oxide to hold the titanium target in place, as this was seen to sag once the titanium became sufficiently hot, resulting in melt of the target prior to aluminium deposition.

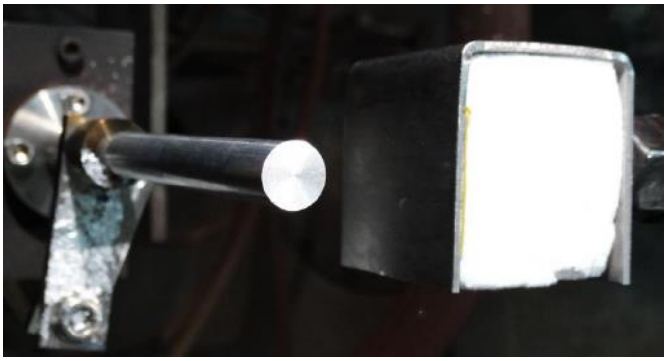

Figure 2: Ejecta Test Setup

The test concept was that the target is heated close to melt by the flow before the sacrificial aluminium part is injected into the flow, at which point it melts and deposits molten material on the surface. This was successfully achieved in two tests. However, there was no noticeable increase in the surface temperature, and the post-test analysis showed a similarly small intermetallic zone as observed in the laboratory testing.

All three stages of the testing, the laboratory tests, the wind tunnel tests and the post-test analysis showed no clear sign of any significantly energy-releasing intermetallic or thermite reactions. There was no clear evidence that the ejecta from molten objects will react with hot unmelted metallic surfaces to release significant amounts of energy which can promote demise. Therefore, it is suggested that this is not considered further as a potential design-for-demise consideration.

3. GLASS MATERIALS

Glasses are amorphous supercooled-liquids, with no long-range periodic structure, and are referred to as supercooled liquids due to the mechanism of formation. Upon cooling of a liquid from temperatures at which it is molten, it will continue to rearrange in terms of structure until the temperature reaches the glass transition temperature, at which point the viscosity has increased by several orders of magnitude, leaving the structure of the material essentially frozen-in, resembling the behaviour of a "solid". If the melt is cooled quickly, such that there is insufficient time for the arrangement of long range crystal structures, the result is an amorphous, supercooled liquid or glass.

Most technologically-relevant and commercial glasses are based on oxide systems. Silica is the most common glass network former. A pure silica glass has high chemical durability and mechanical stability, however, it requires melting temperatures in excess of 2000^{0}C in order to be formable into shapes, so network modifiers such as alkalis and alkaline earths are often added to reduce the melt viscosity for ease of processing.

Glass ceramic materials are obtained by controlled crystallisation of desired phases in bulk glass through the nucleation and growth mechanism during heat treatment. Mechanical properties of glass ceramics are often superior to those of the parent glass, and specific compositions exhibit other distinct properties such as a lower, and potentially tuneable, coefficient of thermal expansion.

Viscosity, the resistance of a liquid to shear deformation with time, is possibly the most important property of glasses and glass-ceramics to discuss when evaluating high-temperature behaviour. The high-temperature viscosity of glass can be estimated using the Vogel-Fulcher-Tammann (VFT) relationship.

$$\log(\eta) = A + \frac{B}{T - T_0}$$

Typical viscosity-temperature relationships are shown in Figure 3.

3.1 Laboratory Testing

Two glass materials have been assessed within this work. These are fused silica, a high purity silicon dioxide glass, which is used in high quality optical instrument lenses, and Zerodur, a commercial glass-ceramic which has a very low thermal expansion coefficient, and is thus used in mirrors for thermal stability. For both of these materials, characterisation of specific heat and thermal conductivity was performed at ÖGI.

As study into the melting behaviour of Zerodur was performed at Sheffield Hallam University. This has demonstrated that the material becomes highly amorphous at temperatures above

1400^{0}C. This corresponds well with the temperatures at which the viscosity of the amorphous glass becomes low enough for significant material removal to occur in re-entry.

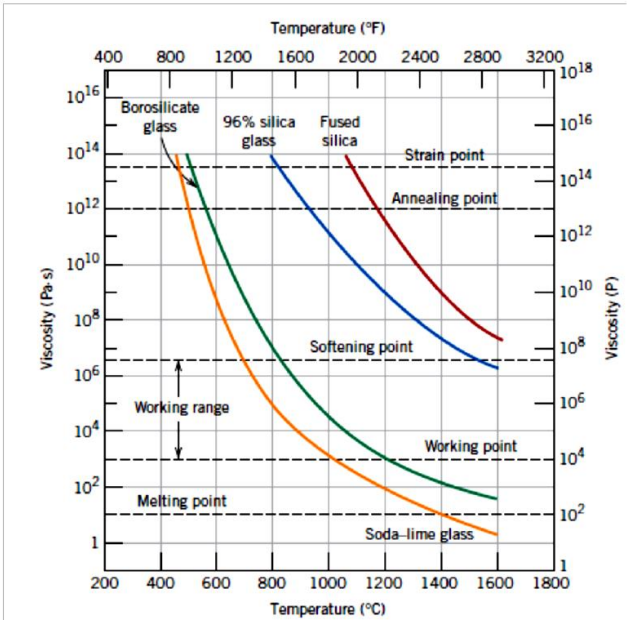

Figure 3: Typical Glass Viscosity-Temperature Curves

The temperature viscosity curve was measured using a rotational viscometer, and the results are shown in Table 1.

Time (mins)	Temperature (°C) (±5)	Log_{10} Viscosity (dPa.s)
0	1300	3.85 (± 0.01)
55	1200	4.45 (± 0.01)
105	1150	4.81 (± 0.03)
150	1350	3.61 (± 0.01)
200	1400	3.39 (± 0.02)
310	1450	3.17 (± 0.02)
350	1500	2.97 (± 0.02)
400	1550	2.77 (± 0.02)

Table 1: Viscosity Data for Zerodur

3.2 Wind Tunnel Testing

Four tests in the DLR L2K wind tunnel were performed on Zerodur, and three on fused silica. The Zerodur tests were performed in two configurations. The first configuration is a stagnation test on a 50mm diameter, 10mm thick sample. These tests show that the viscosity reduces as the temperature rises, and that there is a critical temperature (about 1300^{0}C) where the material begins to move. As the temperature increases, the material moves faster across the surface.

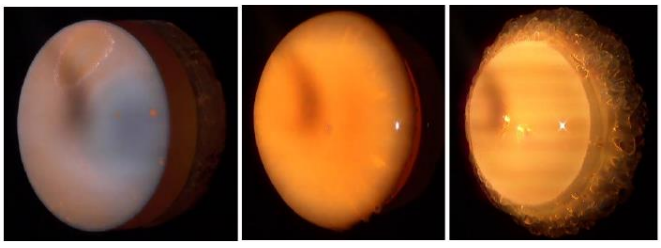

Figure 4: Progress of Zerodur Stagnation Test

As shown in Figure 4, the material gathers at the edge of the sample. This material contains a number of bubbles suggesting that there is some gas release in the decomposition of some of the crystalline components. Some post-test analysis was performed on the sample shown in Figure 5, which showed that the glassy surface was highly amorphous, but the opaque white layer behind was highly crystalline.

Figure 5: Zerodur Sample Post-Test

The rebuilding of the tests using the existent models is shown in Figure 6. This shows that the existent models are far too demisable, and that the predicted temperatures are much too high. This is due to a fully catalytic assumption which is inherent in the majority of destructive re-entry software.

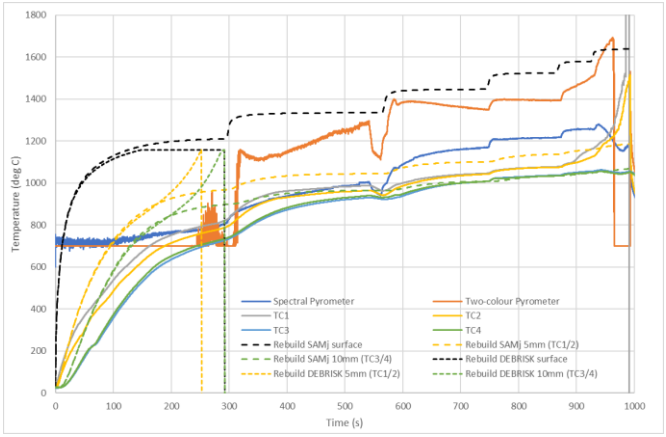

Figure 6: Zerodur Test Rebuild with Original Models

Using the catalycity model in the SAMj tool, a low catalytic recombination coefficient (0.005) can be applied. This is consistent with the findings from silica heat shield assessments, where it is well known that glass materials are close to non-catalytic to recombination of nitrogen and oxygen atoms in re-entry. A much better fit of the temperatures can be obtained with this model as shown in Figure 7. The emissivity used is 0.8, and this provides consistent results.

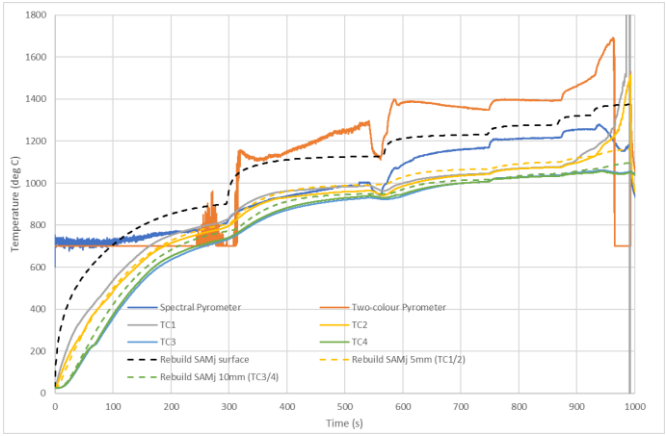

Figure 7: Rebuild with Reduced Catalycity

Tests were also performed in shear mode, as shown in Figure 8. The behaviour observed here was much the same, with the

viscosity reducing as the temperature increases, resulting in the material being able to move across the surface.

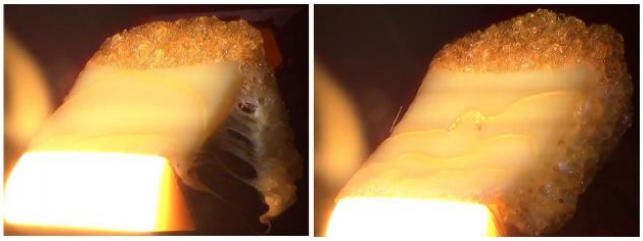

Figure 8: Zerodur Shear Test

As fused silica only reaches low viscosities at much higher temperatures, a different sample was required in order to reach temperatures where some demise could be observed. In order to achieve this, a set of three rods, of 3mm, 6mm and 10mm diameter were used. Figure 9 shows that even though the rods did not reach temperatures at which the material flowed, the smaller rods did become sufficiently hot that they softened to the point where they could bend.

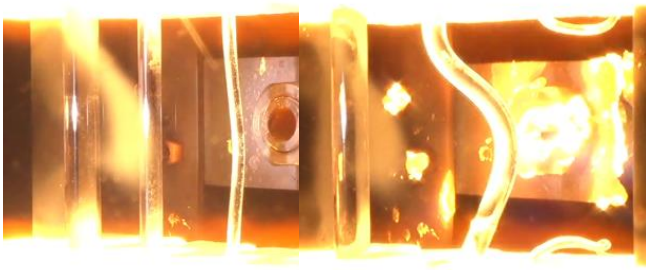

Figure 9: Fused Silica Rods Test

The post-test image of the rods shown in Figure 10, demonstrates that there is no evidence of surface melt, but that the two smaller rods were able to be deformed. The pyrometer data suggests that the surface temperatures of the large rod were of the order of 1600^0C, which is consistent with an emissivity of 0.8 in the numerical rebuilds.

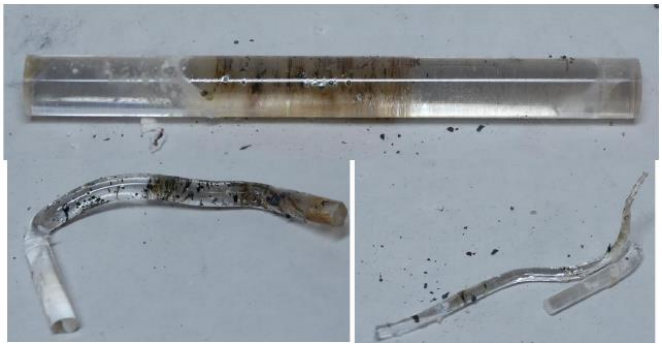

Figure 10: Silica Rods Post Test

The smaller rods reached temperatures in excess of 1900^0C according to the numerical rebuilding, which is clearly beyond the softening temperature, but below the temperature at which the viscosity is expected to reach low enough levels for demise to occur.

An extra test was performed on a large fused silica window (110mm diameter) in order to provide steady state data to assist with the assessment of the catalycity of the material. This test demonstrated that the catalycity was consistent with that of Zerodur, and that the pyrometry readings provided good surface temperature data. This was unexpected as glasses are transparent materials.

3.3 Improved Glass Demise Model

VFT parameters for glass materials of interest are given in Table 2. The parameters in Table 2 are given such that the viscosity is given in Pascal seconds (not Poise), and the temperatures are in Kelvin.

Glass	A	B	T_0
Zerodur	-2.9	6211	496.25
Fused Silica	-2.56	11520	662
Soda Lime	-2.729	4650	213.8
Borosilicate	-2.56	4852	465.5

Table 2: Glass Material VFT Parameters

Prior to the testing performed here, the viscosity level at which shear occurs was essentially unknown. The most appropriate tests for assessing the material removal are the Zerodur stagnation tests as these show the removal of material at close to isothermal surface conditions. This allows the most reasonable assessment of the relationship between temperature, viscosity and surface motion.

A value for the initiation of demise at 1000Pa.s ($\log \eta = 3$) is very close to the onset of material motion as observed in the tests. At this temperature, the material motion was very slow, but was observed to increase significantly as the temperature increased and the viscosity decreased.

The amount of material which can potentially be sheared is given by the depth of the surface layer. This growth rate is close to proportional to the viscosity of the material. Therefore, a reasonable mass loss rate for the demise model of a glass material becomes.

$$\dot{m} = -\frac{m_{layer}}{k\eta(T)}$$

The value of the constant k is determined by fitting the simulation data. A value of 6 has been determined as most appropriate.

This model has been implemented into a Simple Balance Integral (SBI) model which exists within the SAMj tool. This approach performs a two equation assessment of the temperature profile in the material by considering a surface temperature change given by

$$\frac{dT}{dt} = q - \alpha\frac{d^2T}{dx^2}$$

and the bulk temperature, given by

$$\Delta T_{bulk} = \frac{q_{in}A}{mc_p}\Delta t$$

which is standard in demise tools. By imposing a temperature profile of the form

$$T(x) = nx^2 - 2nLx + T_0$$

where T_0 is the surface temperature, L the thickness and

$$n = \frac{T_0 - T_b}{L^2}$$

the temperature through the material can be approximated, and the material removal from the surface can be applied.

Application of this model to the Zerodur stagnation test is shown in Figure 11. The temperatures are reasonably well captured, and the prediction of 90% mass removal is very close to the test data.

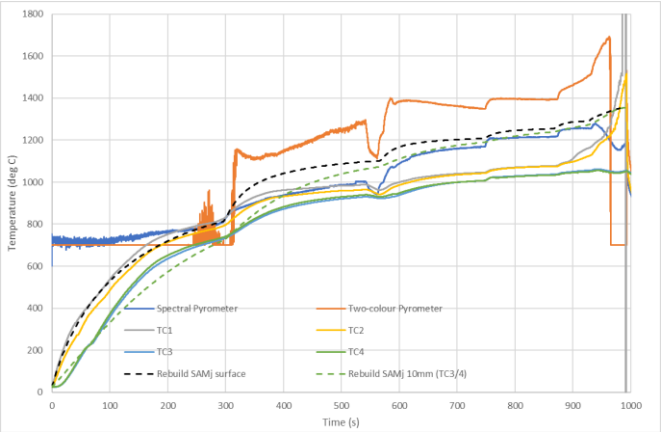

Figure 11: Zerodur Test Rebuild with SBI Model

Extrapolation to flight cases suggests that this model predicts a significantly reduced demisability relative to previous modelling efforts for glasses. This difference is primarily driven by the low surface catalycity, which is not accounted for in most tools.

4. BIPODS

The assessment of bipod demisability is carried out via a reference bipod which has been designed by UCL. This bipod has been designed to support an 8kg mirror, and is sufficiently small to fit in the L2K test section. Variations on this design to improve demisability have been considered, and realised via additive manufacture. All the designs meet the necessary static load requirements.

4.1 Bipod Designs

The reference titanium bipod design is shown in Figure 12. This is a solid design, with the cutouts providing the necessary flexibility for the bipod support.

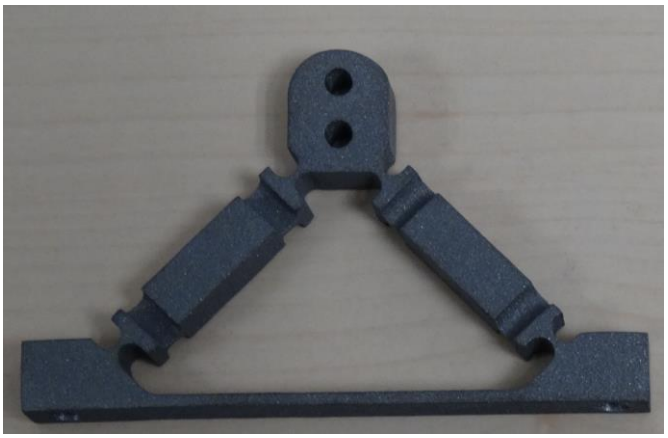

Figure 12: Reference Bipod Design

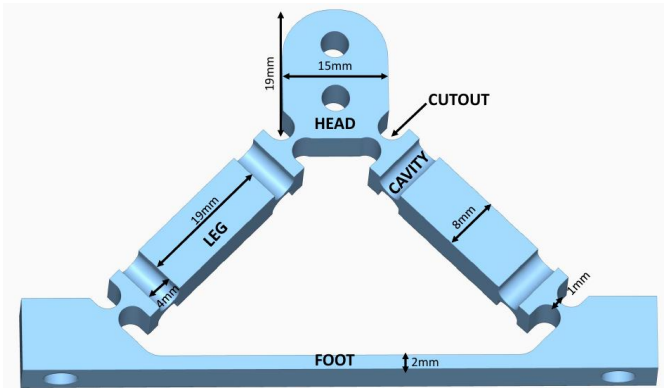

Figure 13: Bipod Critical Length Scales

The presence of the cutouts is important as it results in a range of different length scales of the component, as shown in Figure 13. These different length scales result in the parts receiving significantly different aerothermodynamic heat fluxes, and promote the fragmentation of the bipod in re-entry.

In order to promote demise, two different designs were produced, each employing a different design for demise technique. The first demise improvement was to produce a hollow bipod. Instead of an 8mm thickness, the walls were 2mm thick, and the insides hollow. This design, shown in Figure 14, satisfied the load requirements.

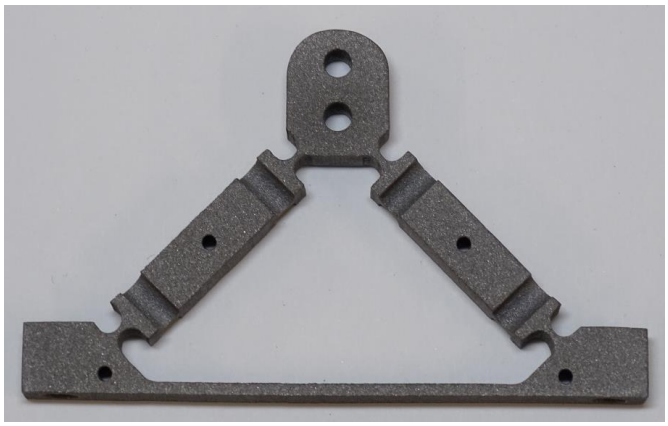

Figure 14: Hollow Bipod Design

The second demise improvement was gained by the addition of flow holes into the structure, as shown in Figure 15. Interestingly, the stress requirements could not be met if the flow holes were manufactured in a solid part, but were satisfied if the part were hollow. All the bipods have been manufactured from titanium.

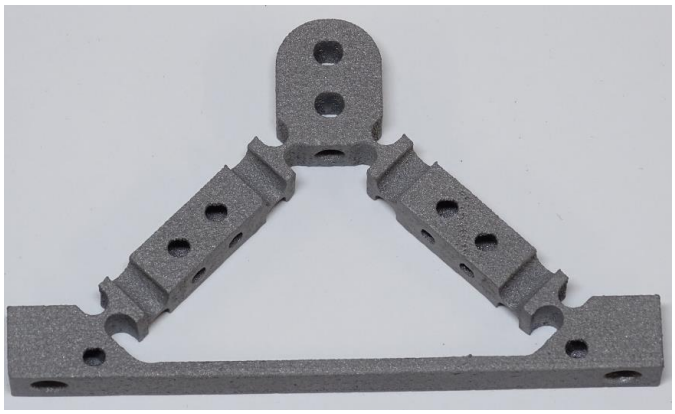

Figure 15: Flow Holes Bipod Design

4.2 Wind Tunnel Testing

Once more, the tests were performed in the DLR L2K facility. As fragmentation was predicted at the cutouts, the samples were held both by the head and one leg in order that the whole sample was not lost. Seven tests were performed in all, with at least one test using the stepped flux approach and a test at constant flux performed for each bipod design.

The tests on the reference bipod demonstrated the importance of the length scale on the heating, as shown in Figure 16. The higher heating at the cutout locations results in the titanium melting at these points and the bipod fragmenting. This suggests that bipods modelled as blocks of the correct volume envelope will underheat in simulation, and that bipods can be significantly more demisable than previously assessed.

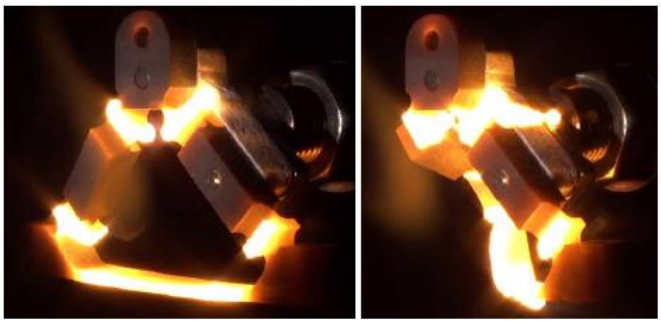

Figure 16: Bipod Length Scale Heating and Fragmentation

Using the correct length scales to rebuild the test data resulted in the heating to the cutouts, foot and legs being very well represented. However, the heating to the head was underpredicted, and the head melted much earlier than anticipated.

As shown in Figure 17, the melt of the head occurred around the upper hole, which had been left open, with the bipod attached to the holder by the lower hole. This suggested that the heating is augmented by flow holes, and led to the addition of holes in one of the designs for increased demise.

Figure 17: Melt of Head at Hole Location

The hollow bipod has a reduced mass relative to the reference bipod, and thus demised more quickly. As shown in Figure 18, the demise process also changed. There is a small hole in the leg to allow the powder from the additive manufacturing process to be removed, and this increased heating can be observed to result in the unattached leg heating nearly as quickly as the cutouts. The fragmentation of the cutouts is similar, but the attached leg demises before the head in this case. The hollow structure results in a significant improvement in the demisability of the legs, and thus the bipod.

Figure 18: Hollow Bipod Demise

The demise is improved further with the addition of flow holes. Figure 19 shows that the heating to the legs is now as rapid as the heating to the cutouts. Numerical rebuilding with SAMj suggests that this is equivalent to reducing the length scale by a factor of 2, thus increasing the heating by $\sqrt{2}$. The legs now demise slightly before the cutouts, showing the increase in demisability.

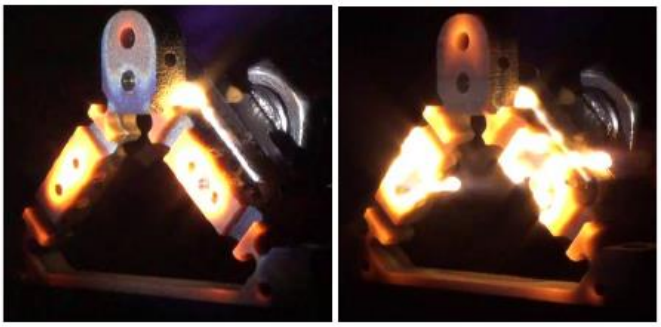

Figure 19: Bipod with Flow Holes Demise

This demonstrates quite clearly that the design for demise techniques applied are highly successful for the bipod. Indeed, the use of flow holes should be a priority for future investigations in demisability improvement.

4.3 Modelling Recommendations

The demise of the bipod was captured well using a multi-component model within SAMj. This is represented in Figure 20. Scaled models of the bipods with masses of 250g and 1.5kg have been run on a re-entry trajectory.

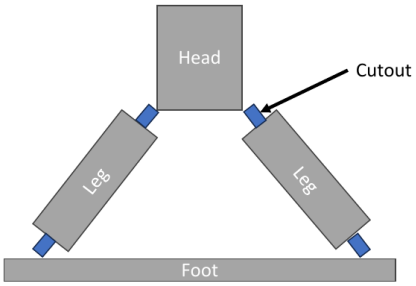

Figure 20: Components in Bipod Model

The larger reference bipods fail due to the demise of the cutouts, and subsequently each of the individual parts demise. This process is similar for the hollow bipods, but the demise is more rapid. However, for the bipods with holes, it is the legs which fail first, mirroring the results from the test campaign.

The demisability of the larger bipods at different release altitudes is given in Table 3. The benefit of the flow holes on the demise of the larger bipod is clear. It is also worth noting that the 250g bipod is demisable in all the cases tested, which would not have been expected for a titanium bipod prior to the test campaign.

Release Altitude (km)	Type	250g Bipod	1.5kg Bipod
78	Reference	Full demise	Full demise
	Hollow	Full demise	Full demise
	Holes	Full demise	Full demise
75	Reference	Full demise	Head survives
	Hollow	Full demise	Head survives
	Holes	Full demise	Full demise
70	Reference	Full demise	Head, legs, foot
	Hollow	Full demise	Head, legs, foot
	Holes	Full demise	Head, foot

Table 3: Bipod Re-entry Demisability

This suggests that capturing of the correct length scale of the bipod parts is more important than representing the envelope in destructive re-entry assessments.

5. CONCLUSIONS

A range of laboratory testing and design work on three aspects of demisability has been performed, culminating in two high enthalpy demisability wind tunnel testing campaigns. These campaigns have demonstrated the demisability of glass materials and bipods, and have investigated the interaction of molten ejecta with hot low-demisability metallic surfaces. From this, a set of modelling recommendations, and an entirely new glass demisability material model have been derived and validated.

The interaction of molten aluminium ejecta with hot steel and titanium surfaces has been investigated in both laboratory and wind tunnel tests. These tests have demonstrated that there is very little evidence of intermetallic or thermite-type reactions, and that this is unlikely to be a source of heat which can be used in designing for demisability. Indeed, the effect is sufficiently small that it is not recommended to include this in destructive re-entry assessments, and it is considered that no further investigation into the phenomenon is necessary.

The demise of glass materials has been demonstrated clearly to be driven by the surface viscosity of the material, for both glass and glass-ceramic materials. New data for the specific heat capacity, conductivity and viscosity of Zerodur have allowed the test data to be rebuilt and the mass loss to be captured by a novel modelling approach. This simplified heat balance integral approach is appropriate for implementation in DRAMA. Proxy models have also been constructed to partially capture the demise behaviour of glass materials using the current DRAMA capability.

The demise behaviour of bipods has been assessed using a baseline design of a titanium bipod, targeting use with an 8kg mirror. The bipod design, which involves thin structures and cutouts has been demonstrated to be significantly more demisable than would be captured by standard models. Fragmentation at the cutouts is clearly observed in the tests, which suggests that critical aspects of bipod demisability are not generally modelled. From the results of the baseline bipod tests, enhanced designs with hollow parts and flow holes were produced and manufactured using 3D printing. The hollow design was more demisable due to the reduced mass of the material, and the flow holes provided a significant increase in the demisability due to the change in the shock shape. This resulted in a significant reduction of the effective length scale, and the use of holes is highly recommended for further study as a design-for-demise technique. A set of recommendations for the modelling of bipods has been made, both in terms of the model construction, and modelling tool capability. Capturing the correct length scale and improving the fragmentation representation are the key aspects.

Overall, this has been a successful design testing and modelling activity which has produced new data, and new models which are recommended to be implemented into destructive re-entry tools for ground casualty risk assessments.